Supplementary Data

The nuclear export factor CRM1 controls juxta-nuclear microtubule-dependent virus transport

I-Hsuan Wang, Christoph J. Burckhardt, Artur Yakimovich, Matthias K. Morf & Urs F. Greber

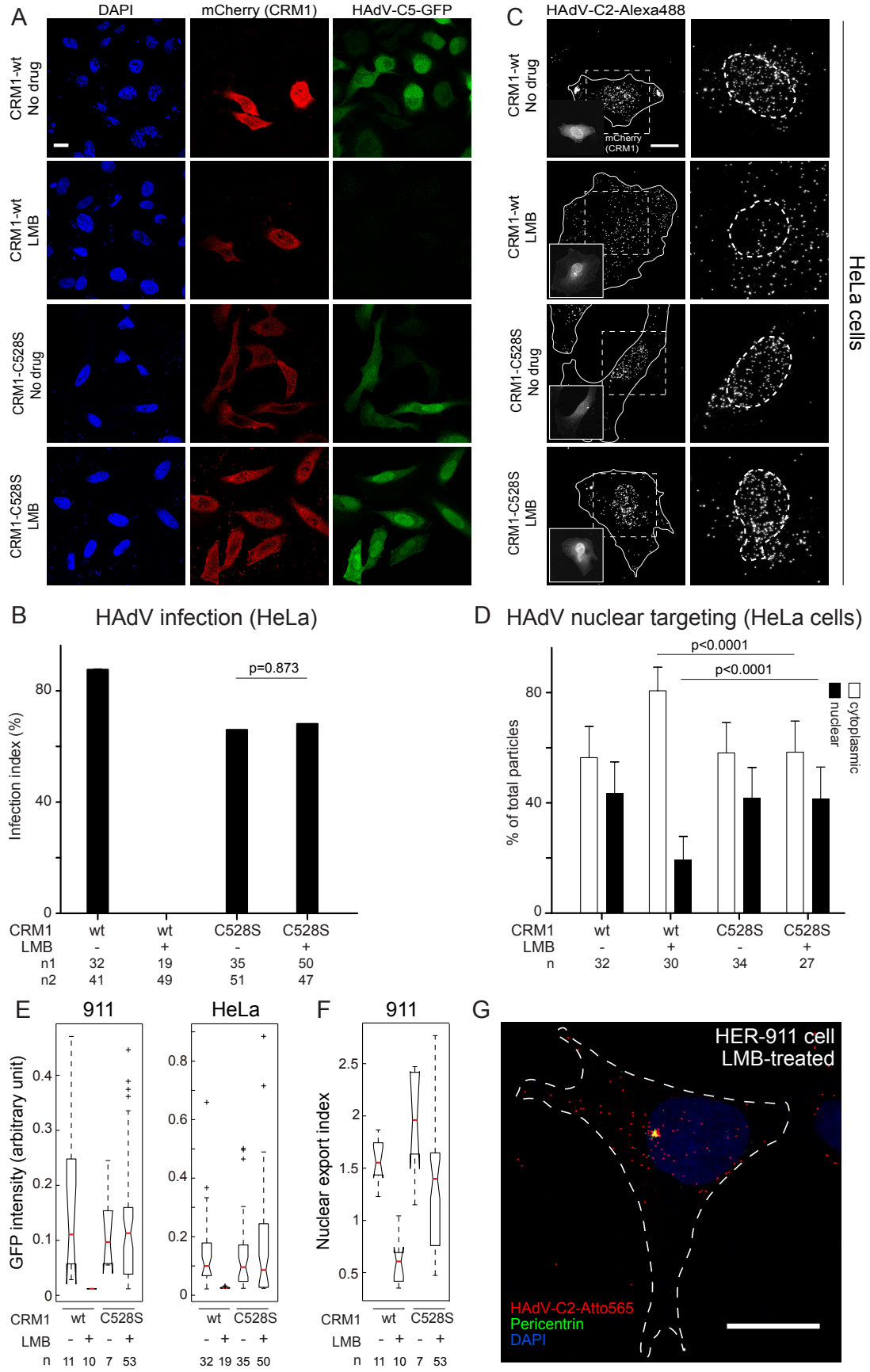

Fig. S1: Rescue of adenovirus nuclear targeting and genome delivery in LMB-treated HeLa and HER-911 cells expressing LMB-resistant CRM1 (related to Fig. 1).

A) HeLa cells were transfected with CRM1-wt-mCherry or CRM1-C528S-mCherry and treated with or without LMB, followed by inoculation of HAdV-C5_GFP for 16 h. Scale bar = 20 µm.

B) Representation of infection indexes based on the percentage of infected (GFP positive) transfected cells, including the p-value between LMB and control cells transfected with the LMB resistant mutant CRM1-C528S-mCherry. The experiment was conducted twice, and the numbers of cells analyzed in each biological replicate are indicated (n1, n2).

C) Examination of the nuclear targeting of incoming HAdV-C2-Atto647 particles in CRM1-wt-mCherry and CRM1-C528S-mCherry expressing HeLa cells 90 min pi. The transfected cells are displayed in the inset with white outline. The dashed lines in the blown-up images in the right row indicate the nuclear region. Scale bar = 20 µm.

D) Quantification of HAdV-C2-Atto647 nuclear targeting. Mean values of the subcellular localization of the virions at the nuclear membrane and in the cytoplasm, including the standard deviations and number of cells analyzed (n).

E) Representative data sets of HAdV-C5_GFP infections. The notched boxplots show the 25^{th} to 75^{th} percentile and median of data points. Outliers, which are 1.5 times the interquartile range (indicated by the whisker) away from the edge of the box, are represented by the plus signs.

F) Assessment of nuclear export of endogenous Rio2 in HER-911 cells transfected with CRM1-wt-mCherry or CRM1-C528S-mCherry, in presence or absence of LMB.

G) Representative image of incoming HAdV-C2-Atto565 particles arrested at MTOC upon LMB treatment in HER-911 cell 90 min pi. The MTOC was immunolabeled by an anti-pericentrin antibody. The dashed line indicates the outline of the cell. Scale bar = 20 µm.

Journal of Cell Science • Supplementary information

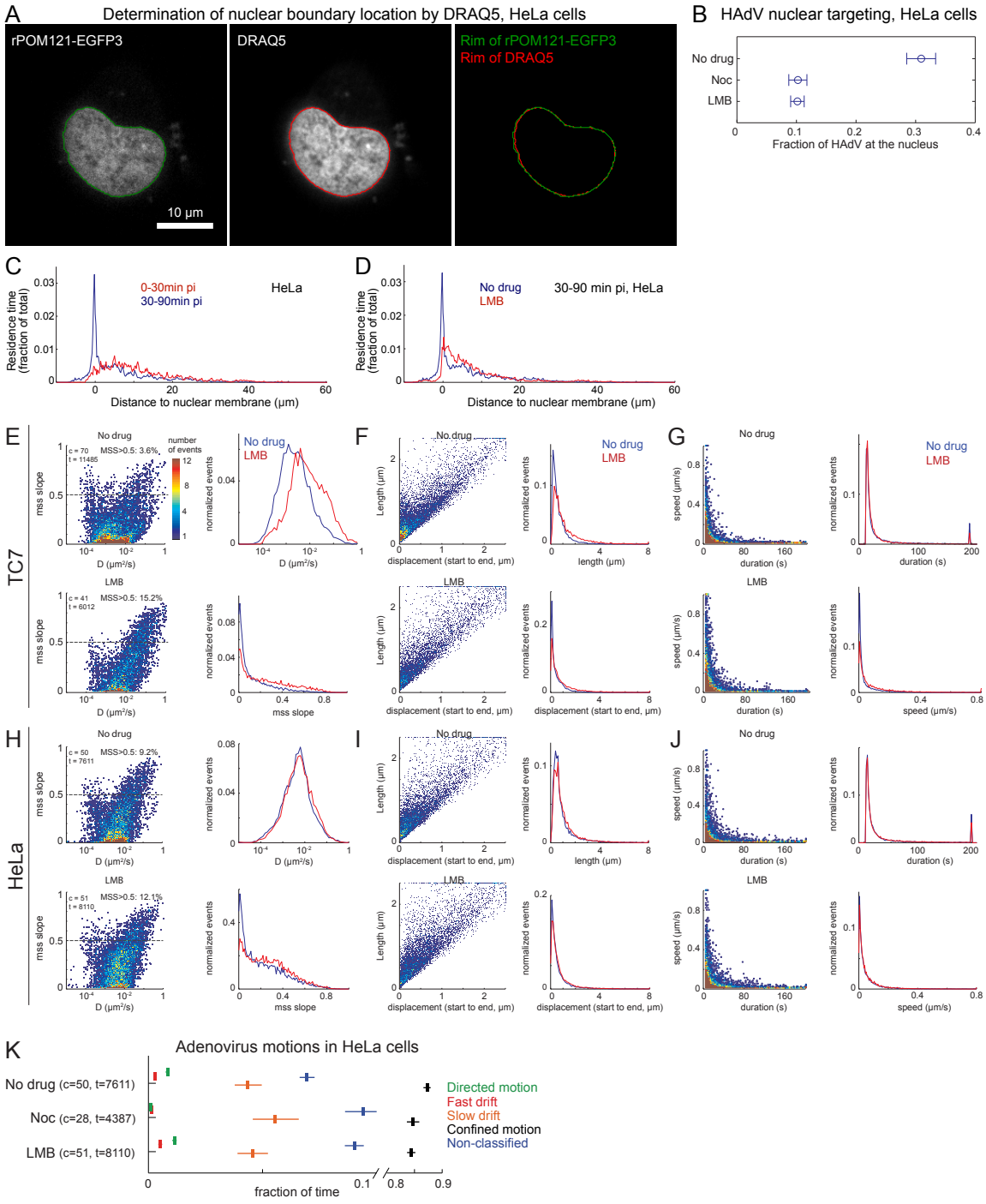

Fig. S2: Analyzing the subcellular localization of viruses by live cell imaging in HeLa and TC7 cells (related to Fig. 2).

A) To validate the delineation of the nuclear rim determined by DRAQ5 in fixed specimens, TC7 cells were transfected with rPOM121-EGFP3, and stained with DRAQ5 in live mode. The boundaries of the rPOM121-EGFP3 and DRAQ5 signals were

determined and compared with each other using the same procedures as for the fixed cells. The results show a high degree of overlap between the POM121 and the DRAQ5 nuclear rims.

B) Analyses of HAdV-C2-Alexa565 located at the nuclear membrane in HeLa cells upon treatment with LMB or nocodazole (Noc) 30-90 min pi.

C) Residence time of HAdV-C2-Alexa565 in relation to the distance of the virions from the nuclear membrane in the time windows 0-30 min and 30-90 min pi.

D) Distance plot of residence time of HAdV-C2-Alexa565 in presence or absence of LMB, 30-90 min pi.

E, F) Characterization of adenovirus movements in infected TC7 and HeLa cells by frequency plots of mss slopes and diffusion constants of virion trajectories, and histogram profiling in control cells (blue) and LMB-treated cells (red). Events with mss slopes >0.5 represent active transport, 0.5 random walk (dashed line), and <0.5 restricted diffusion. The number of cells (c) and virus tracks (t) analyzed are indicated for each panel.

G, H) Frequency plots of trajectory run lengths and overall displacements of virions. Note the indication of the relative occurrence of motion periods with an MSS-slope larger than 0.5, that is, with a high component of linear motion (panels E and H).

I, J) Frequency plots of speed and duration of virion movements.

K) Abolishment of adenovirus directed motions and fast drifts in HeLa cells by nocodazole. Representation of the median time, for which virions engaged in directed motion (DM, green), fast drift (FD, red), slow drift (SD, orange), diffusion (cyan), confined motions (CM, black) and not classified (NC, dark blue) including 95% confidence intervals (horizontal bars) obtained by bootstrapping. Results are expressed as a fraction of total time analyzed for each condition, and include the number of cells (c), and the number of virus trajectories (t).

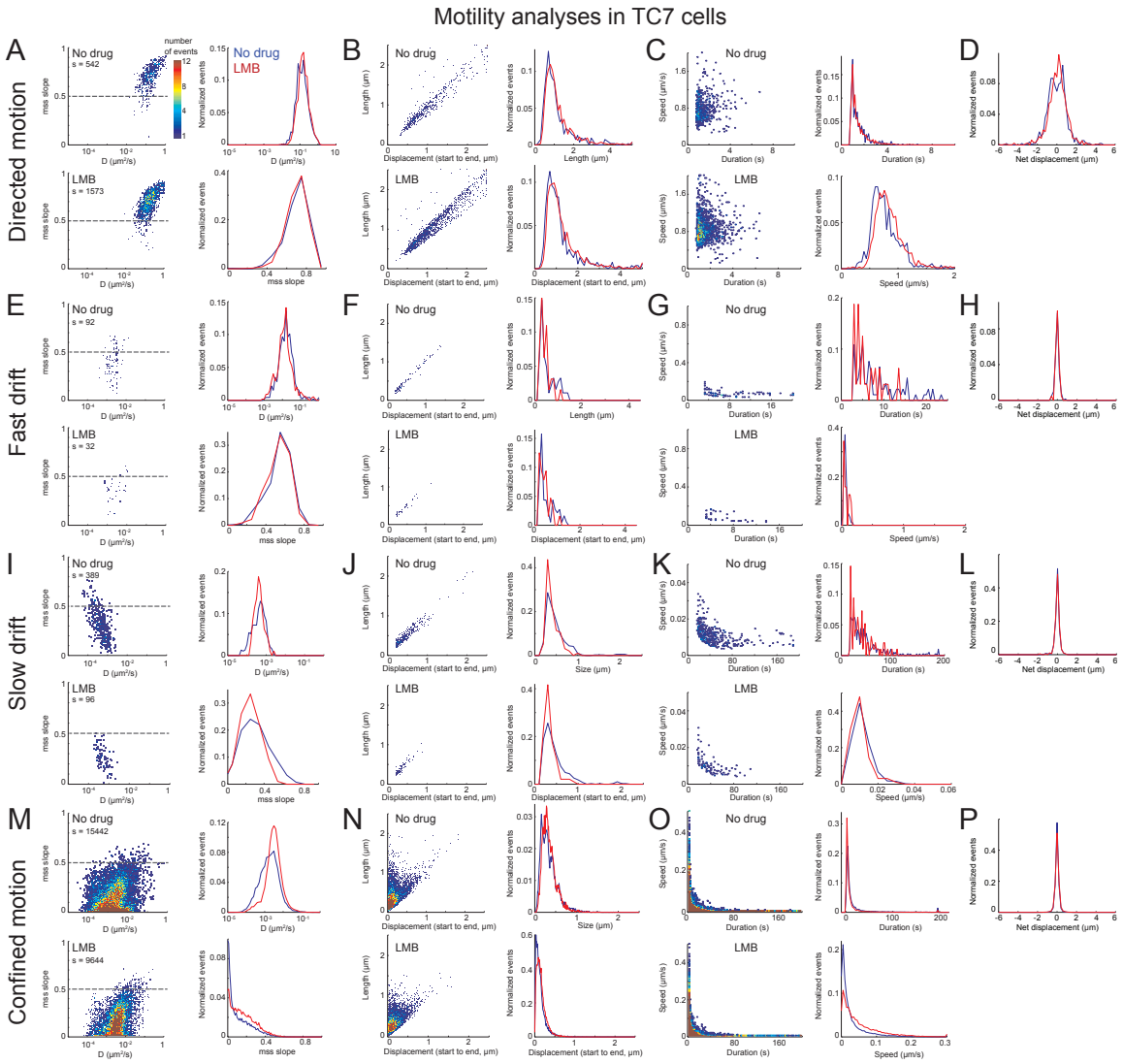

Fig. S3: Features of virion motions in TC7 cells (related to Fig. 2).

The virion trajectories from control and LMB-treated cells were segmented and categorized into directed motion (**A-D**), fast drift (**E-H**), slow drift (**I-L**), and confined motion (**M-P**). Each motion type was analyzed for its mss slope (**A, E, I, M**), run length (**B, F, J, N**), duration (**C, G, K, O**) and directionality (**D, H, L, P**). The distribution of these parameters was plotted and compared between control (blue) and LMB-treated cells (red), including the number of segments analyzed (s).

Journal of Cell Science • Supplementary information

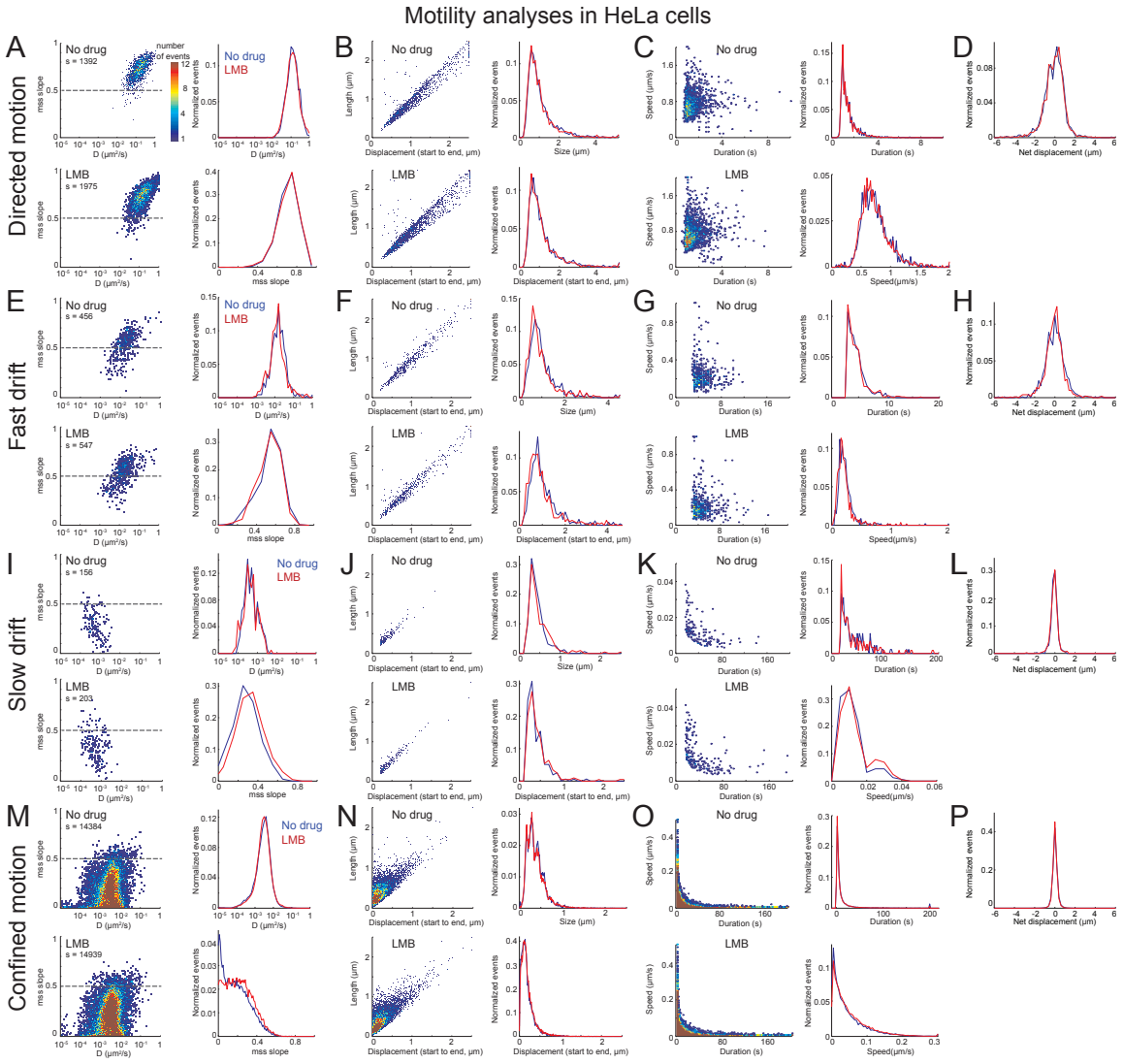

Fig. S4: Features of virion motions in HeLa cells (related to Fig. 2).

The virion trajectories from control and LMB-treated cells were segmented and categorized into directed motion (**A-D**), fast drift (**E-H**), slow drift (**I-L**), and confined motion (**M-P**). Each motion type was analyzed for its mss slope (**A, E, I, M**), run length (**B, F, J, N**), duration (**C, G, K, O**) and directionality (**D, H, L, P**). The distribution of these parameters was plotted and compared between control (blue) and LMB-treated cells (red), including the number of segments analyzed (s).

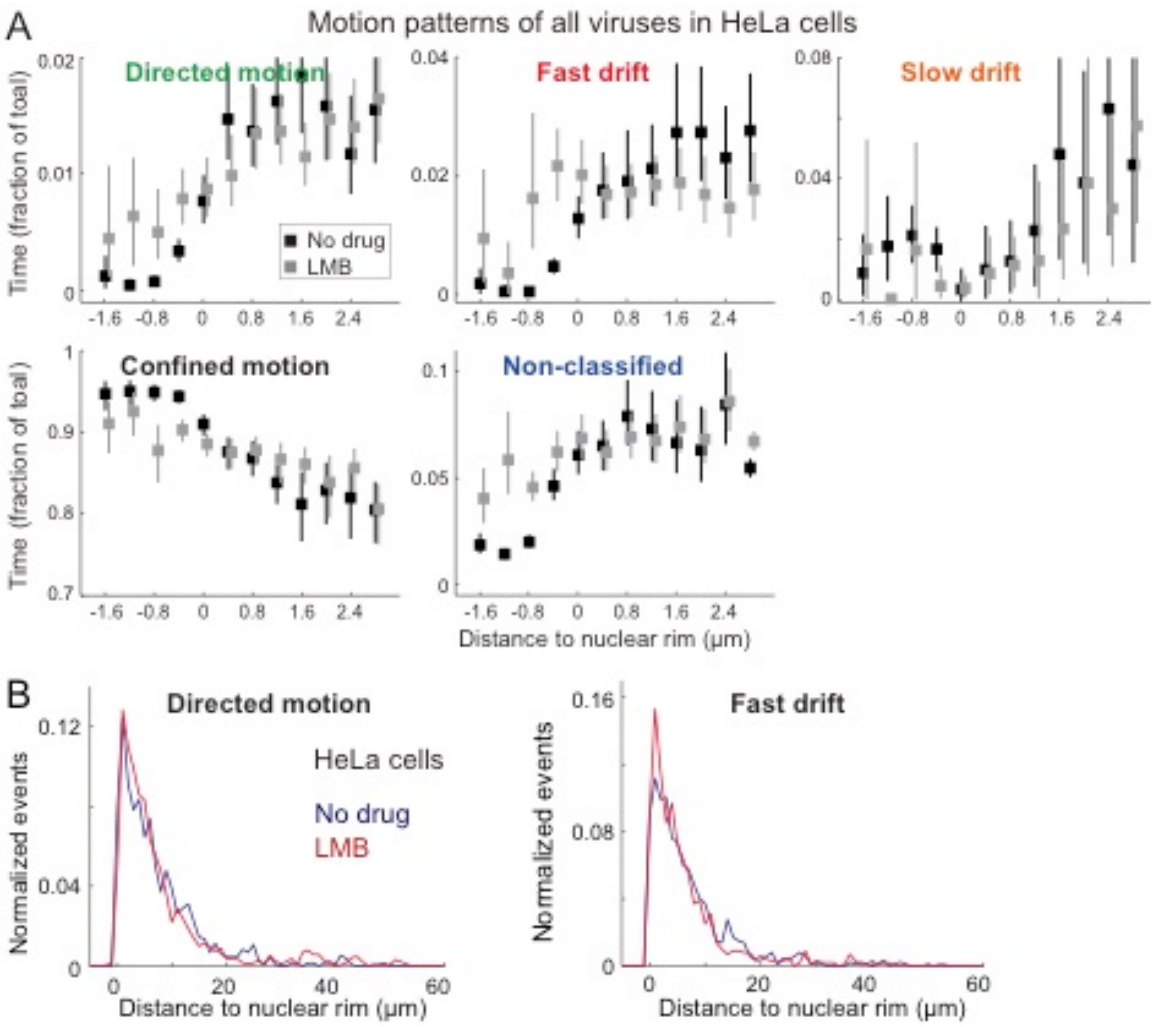

Fig. S5: CRM1-sensitive motion gradient of adenovirus in HeLa cells (related to Fig. 4).

A) Virion motions in relation to their distance from the nucleus in the zone -1.6 µm to 2.8 µm around the nuclear rim. The nuclear rim is positioned at 0. Negative distance values indicate overlap with the nuclear mask, and positive values indicate motions in the cytoplasm distant from the nucleus. Events were binned into 0.4 µm segments, and results plotted as the median time of virions in each motion type. Results from control cells are represented in black, and LMB-treated cells in grey squares.

B) Subcellular localization of the starting points of the DM and FD across the entire cytoplasm of control and LMB-treated cells.

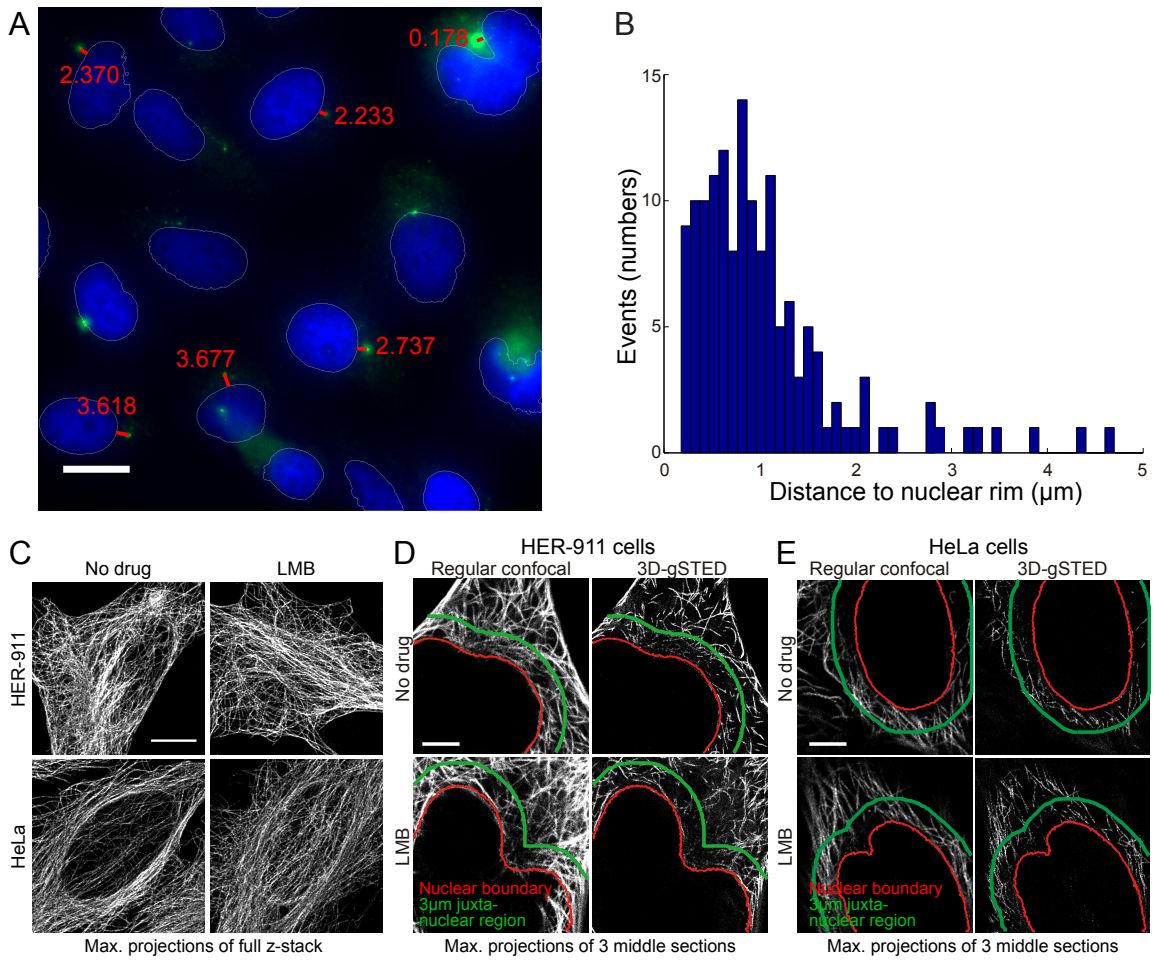

Fig. S6: Distance profiling of the location of the MTOC with respect to the nuclear membrane and microtubule morphology in the perinuclear zone (related to Fig. 5).

A) A representative image of the microtubule organizing centers (MTOCs) stained with an anti-pericentrin antibody (green), and DAPI-stained nuclei (blue) as a reference in HER-911 cells. The distance between the MTOC and the nuclear rim (white line) is indicated by a red line and a corresponding red number in μm. Scale bar: 20 μm.

B) Histogram showing the frequency of MTOC location with respect to the nuclear rim.

C) Morphology of the microtubule network in HER-911 and HeLa cells. Control or LMB-treated cells were stained for β-tubulin, imaged by confocal fluorescence microscopy, and displayed as maximal projections of deconvolved image stacks. Scale bar = 10 μm.

D, E) Three z-sections of microtubule-stained HER-911 (B) and HeLa (C) cells were acquired at the middle of the cells in 3D-gSTED mode of the confocal laser scanning microscope. The maximum projections were created from image stacks. Scale bar = 5 µm.

MovieS1

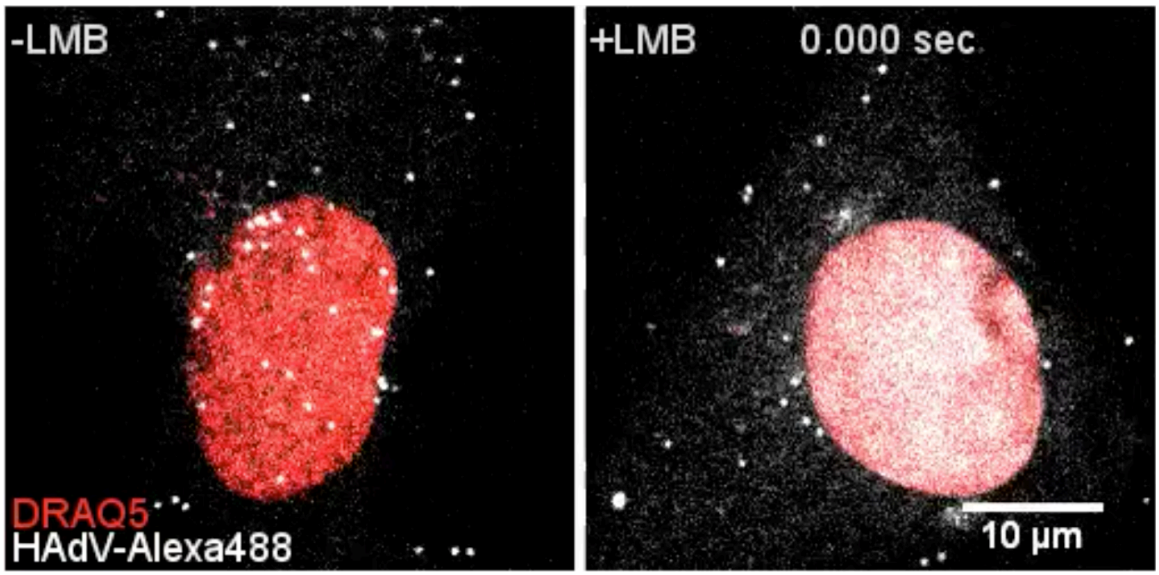

Supplementary Movie 1: Motility of adenovirus particles in control and LMB-treated TC7 cells.

Control or LMB-treated TC7 cells stained for DNA with DRAQ5 were warmed for 30-90 min from cold-synchronized inoculation of HAdV-C2-Alexa488 (white), and imaged by spinning disc confocal microscopy at a frequency of 25 Hz. For details about the procedure, see main text.